Enhancement the Properties of Ni Compisite Electroplated Using Nano-Chromium Oxide Powder

Z. Abdel Hamid[1] and S.M. El-Sheikh[2]

[1]Prof. Zeinab Abdel Hamid, corrosion control and surface protection department, Central Metallurgical Research & Development Institute, CMRDI, P.O.87 Helwan, Cairo, Egypt. Fax: +20225010639, Tel: +201223405792, E.mail: forzeinab@yahoo.com

[2]Nano structured material and nano technology department, Central Metallurgical R & D Institute (CMRDI) Cairo, Egypt

Abstract

Nickel electroplating is one of the few surface finishing processes that can satisfy the requirements of decorative and functional applications. In this work, nickel composite coatings containing nano–Cr2O3 particles were produced by conventional electroplating (CEP) technique from nickel-Watt's type bath. Nano-Cr2O3 powders were synthesized by sol-gel technique. The influence of plating parameters including current density, pH, stirring rate, temperature and nano-Cr2O3 concentrations in the plating solution on the volume fraction (Vf %) of the co-deposited Cr2O3 particles in Ni-matrix was investigated. The results demonstrated that the Vf % of Cr2O3 particles incorporation in the deposited layer depends on these operating conditions. The maximum value of co-deposited nano- Cr2O3 can be achieved at optimum conditions; 20 g1-1 of Cr2O3 particles in suspension, 7Adm-2, pH 5, a stirring rate 150 rpm and 50 °C. The morphology of composite coatings was investigated using scanning electron microscopy (SEM). The results showed that the incorporation of nano-Cr2O3 particles changed the surface morphology of nickel matrix. The properties of the composite such as hardness and corrosion resistance were examined compared with steel uncoated and coated with nickel. The results revealed that the presence of nano-Cr2O3 particles in Ni-matrix greatly improved the hardness and corrosion resistance of steel.

Keywords

Coatings, Composite Materials, Electroplating, Ceramic Particles, and Nano-composite

Introduction

Electroplating is the application of electrolytic cells in which a thin layer of metal is deposited onto an electrically conductive surface. Nickel electroplating enhances the appearance, extends the life and improves the performance of both materials and products in different environments. The presence of fine particles in a metal matrix generally improves its mechanical and chemical properties such as hardness and wear resistance and corrosion resistance relative to the pure matrix (Sarret M. etal. 2006). Composite materials can be defined as coatings consisting of minute particles dispersed throughout a metal matrix. Composite coatings have been used in various industries such as, jet engines seals, aeronautical, marine, mining, agriculture and nuclear fields. However, the magnitude of the benefit depends on their volume percentage. Due to increasing demand in more compact designs, better reliability, lower fuel, lube or material consumption in most advanced tribological systems, the nanostructure compact coating is preferred to achieve better durability and high performance. The unique functional properties of the coatings are derived from the presence of particles dispersed in the metallic matrix and sometimes from the particles themselves which are only partially engulfed at the coating surface (Sarret M. etal. 2006, Rossi S. etal. 2003, Ramesh Bapu G.N.K., 1994).

Various engineering ceramics, such as SiC, TiC, Al_2O_3, TiB_2, B_4C, …, etc., are commonly used today as reinforcement phase (Qiuyuan F. etal. 2008, Berkh O. etal. 1995, Abdel Hamid Z. etal. 1999). In an earlier works, electroless Ni–P composite coatings incorporated into ZrO_2, TiO_2 and Al_2O_3 on 6061 Al alloy have been studied (Abdel Hamid Z. etal. 2002). In addition, electrodeposited Ni-P composite coatings incorporated into a variety of ceramic particles were investigated from Ni-Watt's bath (Shawki S. etal. 1997, Wahi R.P. etal. 2005, Zhang C. etal. 2005, Abdel Aal A.

etal. 2007). The mechanism of co-deposition of various particles (SiC, Al_2O_3, quartz and sand) was studied in view of the electro-kinetic charge characterizing the solid particles.

With the emergence of nanostructure materials over the last decade, electrodeposition techniques have provided a route for a variety of new nanomaterials including nanocrystalline deposits, nanowires, nanotubes, nanomultilayers and nanocomposites. The nanostructure composite coatings possess excellent wear protection especially lower friction and wear loses and increased resistance towards fatigue. These coatings are extremely hard and tough in comparison with the conventional coatings. These nanostructure coatings are capable to improve the performance of some of the mechanical components in various industrial applications as well as to increase the resistance towards deformation even in heavily loaded rolling or rotating contacts (Abdel Aal A. etal. 2007).

Accordingly, in the present work, nanometer-sized Cr_2O_3 particle-reinforced Ni matrix composite coatings (Ni–Cr_2O_3) were prepared by conventional electroplating (CEP) technique from Ni-Watt's bath. The objective of this study is to investigate the effects of the electroplating parameters such as concentration of Cr_2O_3, current density, pH, stirring rate and temperature on the quantity of nanosized particles incorporated into the metallic deposit. Scanning electron microcopy (SEM) was used to investigate the surface morphology of Ni–Cr_2O_3 films deposited at different operating conditions. Hardness and corrosion properties of composite coatings have been investigated and compared with uncoated and coated steel with nickel.

Experimental

Preparation of Cr2O3 Powder

The chromium oxide, Cr_2O_3, used in this study was pure Cr_2O_3 powder (99.5%) with particle size 36nm. Cr_2O_3 nanopowders, were obtained by a sol–gel method. Chromium oxide nanopowders have been obtained via the reduction of $K_2Cr_2O_7$ (PDC) by maleic acid. Maleic acid was added to 1.7M PDC solution at pH 7 and at room temperature. The resulting solution was stirred for 24 hr, and left for 15 days to form a green gel which was separated by filtration and washed with de-ionized water three times. Then the gel was kept at room temperature for about 24 hr, followed by heating at 110°C for about 24 h. Morphology of the sample is investigated using transmission electron microscopy (TEM, JEOL-JEM-1230, Japan) as shown in Fig. 1.

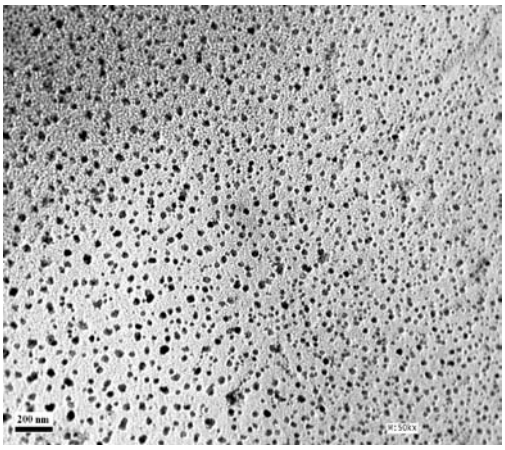

FIG.1TEM IMAGE OF THE AMORPHOUS CR_2O_3 PARTICLES.

Electrodepositing Process

Coatings were obtained on mild steel substrates as a cathode with dimension 40 × 40 × 0.6 mm and its chemical composition is shown in Table 1. Deposition was performed after a suitable pre-treatment sequence including degreasing using an aqueous alkaline solution, then immersed in 10% v/v HCl for 1 min. The anode was a pure Ni plate. The nano-Cr_2O_3 particles were pretreated with acetone to remove residual organic, before adding to the plating solution, then washed with distilled water and dried. Prior to the co-deposition, the Cr_2O_3 particles were stirred using magnetic stirrer to get uniform suspension of particles in the solution and prevented agglomeration. CEP technique from Watt's bath was used to prepare Ni and composite coatings. The bath contains nickel sulfate 250 gl^{-1}, nickel chloride 45 gl^{-1}, and boric acid 30 gl^{-1}. Analytical reagents and de-ionized water were used to prepare the plating solution. During electrodeposition the applied bath was operated at pH (3–7), stirring rate (50-250 rpm) and temperature (25–70°C). For pH-dependent experiments the pH was adjusted by the addition of either NH_3 solution or H_2SO_4. The prepared powder Cr_2O_3 was dispersed into plating solution with different concentrations (0–30 gl^{-1}). After steel treatment it was immersed in Ni plating bath containing suspension of Cr_2O_3 powder. The coated samples were washed and dried. The volume fraction of embedded Cr_2O_3 particles in the coating layers was evaluated by the use of point counting technique with the help of SEM. The determined

amount of codeposited Cr_2O_3 in the Ni matrix resulted from the mean value of at least three measurements for each deposit. The detailed method is explained elsewhere (Pickering F.B. 1976).

TABLE 1 CHEMICAL COMPOSITION OF MILD STEEL SHEET

Element	C	Mn	Si	S	P
wt%	0.15	0.6	0.25	0.025	0.028

Zeta Potential Measurements

A laser zetameter 'Malvern Instruments Model Zetasizer 2000' was used for zeta potential measurements. 0.02 g of Cr_2O_3 particles was placed in 50 mL double distilled water, and pH modifier having ionic strength of $2X10^{-2}$ M KCl. The suspension was conditioned for 3 h during which the pH was adjusted. The pH was then adjusted to the required value. The sample was shaken for one hour. After shaking, the equilibrium pH was recorded. It was then allowed to settle for 3 min, and ≅10 mL of the supernatant was transferred into a standard cell for zeta potential measurement. Solution temperature was maintained at 25 °C. Ten measurements were taken and the average was reported as the measured zeta potential (El-Reheim F. H. A etal. 2008).

Characterization of Composite Layers

The degree of adhesion performance between the film and the steel surface was investigated by scratch test. In this method, six parallel cuts were made on the test panel by a cutting tool (Multi-blade) with six cutting edges spaced 1 or 2 mm apart. Adhesion tape (AME Ricav Tape) was applied firmly to the cut area and then removed rapidly by pulling at right angles to the test panel. According to international standards ISO 2409, the coating adhesion was classified into six classes. In addition, the degree of adhesion for the deposited layer with the steel surface was investigated using thermal shock test. In this test, the samples were heated in the muffle furnace. When the temperature of the furnace reached up to 650 °C in air, the samples were pushed into the furnace for 24 h then quenched into the water. Before and after the thermal test the coated layer was examined using an optical Oplympus BX41M microscope provided with video camera to estimate the failure of the coating.

The characterization of the deposits morphology was performed using scanning electron microscopy (SEM) model JEOL, JSM-5410. Measurements of the vickers microhardness (Hv) of pure steel and coated steel acting as a substrate were performed on their surface using Tukon Series B200 Microhradness Tester by applying a 100 g load with diamond pyramid indenter technique for indentation 30 s and the corresponding final values were determined as the average of 10 measurements. The thickness of the coatings (30 μm) and the selected load were chosen so as to avoid any substrate effect on the measured microhardness value. The phase structure of the films was characterized by X-ray diffraction analysis using Bruker AXS X-ray diffractometer with Cu Kα1 target of wavelength 0.15046 nm. The corrosion rates of uncoated and the coated steel in 3.5 % NaCl solutions were investigated with an immersion weight loss technique. This test is the most economical mean to provide a preliminary selection of the best suited materials. The immersion test is the cyclic test procedure where a test specimen is immersed for a period of time in a test environment, then removed, dried and weighed before being re-immersed to continue the cycle. The experiments were carried out at normal room temperature and corrosion time 120min.

Results and Discussion

The inclusion of nanosized particles into metal matrix deposits is dependent on many process parameters such as, particle concentrations, surface charge, temperature, pH, stirring rate and current density.

Effect of Nano-Cr2O3 Concentrations

The previous studies were confirmed that the codeposition of ceramic particles smaller than 100 nm with metal matrix was more difficult than that of submicron (Abdel Aal A, 2006, Maurin G etal., 1995). The effect of the nano-Cr_2O_3 concentrations in the plating bath on the deposition behavior of the Ni-Cr_2O_3 composite coating layer was investigated. Electrolytic codeposition of nano-Cr_2O_3 with nickel was carried out at current density 7 Adm^{-2}, 50 °C, 150 rpm, and pH 5. Figure 2 shows the influence of Cr_2O_3 concentrations in the plating bath on the V_f % of nano-Cr_2O_3 particles in the nickel matrix. It is clear that the particles inclusion in the coating layer depends heavily on the amount of suspended particles in the electrolyte. The V_f% of Cr_2O_3 particles in the deposit increases sharply with the increasing concentration of Cr_2O_3 in the electrolyte and attains the optimum value at 20 gl^{-1} and then decreases with further increasing Cr_2O_3 concentration in the plating bath. This means that the entrapment of the Cr_2O_3 particles into the growing nickel matrix depends on the rate of Cr_2O_3

particles approaching to the cathode surface. The maximum V_f% of the Cr_2O_3 particles may correspond to steady state equilibrium, where the number of codepositing particles equals that number approaching the cathode surface. Beyond the optimum concentration (20 gl^{-1}), suspended particles appeared to agglomerate in the bath. Accordingly, the decreasing trend of incorporation of Cr_2O_3 particles into the nickel matrix was observed. This trend may be explained on the basis that, at high suspension concentration the agglomerates themselves will be resistant to incorporate and shield the surface from the flux of incoming particles (Hou K. H etal. 2002). The more Cr_2O_3 particles content there were in the plating bath, the higher viscosity of the plating solution was, therefore, the experimental was restricted to the Cr_2O_3 concentration in the plating bath (20 gl^{-1}).

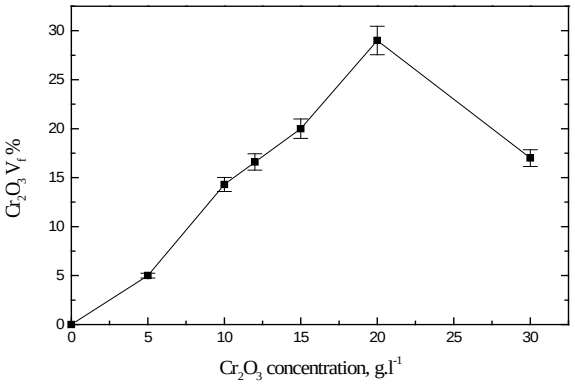

FIG.2 RELATIONSHIP BETWEEN Cr_2O_3 Concentration In The Electrolyte AND V_f % Of Cr_2O_3 PARTICLES IN THE DEPOSITED LAYER OPERATED AT 7 ADM^{-2}, 150 Rpm, pH5 AND 50 °C.

Moreover, the curve is quite similar to the well-known Langmiur adsorption isotherms, supporting a mechanism based on an adsorption effect. Codeposition mechanisms for the dispersion of inert particles into metallic coatings have been developed from investigations of micron sized particles (Shawki S etal. 1997, Guglielmi N, 1972, Bercot P etal. 2002, Fransaer J etal. 1992, Balaraju J.N etal. 2003, Celis J. etal. 1990, Celis J. P etal. 1991, Zhong-jia H. etal. 2008). The mechanism proposed by Guglielmi (Guglielmi N, 1972) has been adopted by various authors. So, the codeposition of Cr_2O_3 by the electrodeposition technique may be attributed to the adsorption of Cr_2O_3 particles on the cathode surface as suggested by Guglielmi's and elsewhere (Shawki S etal. 1997, Hou K. H etal. 2002).

Figure 3 shows the SEM surface morphology of pure Ni and Ni-Cr_2O_3 deposited from baths containing different Cr_2O_3 concentrations and operated at 7Adm^{-2}, 50°C, 150 rpm, and pH 5. Nano-Cr_2O_3 particles are distributed in the deposit as white spherical globules. It is clear that, the shape of Ni crystallites is regular pyramidal crystals as shown in Fig. 3a. The distribution of the Cr_2O_3 particles on the cathode surface increases with increasing amount of suspended Cr_2O_3 in the bath. At 5 gl^{-1} Cr_2O_3 particles in the plating solution, 5 V_f % of Cr_2O_3 was found as seen in Fig. 3 b. With further additions of Cr_2O_3, the spreading of Cr_2O_3 increased as shown in Fig. 3c-f. Maximum coverage of the nickel matrix with Cr_2O_3 was obtained at 20 gl^{-1} and corresponding incorporation was around 29 V_f % (Fig. 3f). As can be seen, the surface of nickel coating observed under a scanning microscope is made up of regular pyramidal crystals with an uniform grain size (Fig.3a). The codeposition of nanosized particles Cr_2O_3 in a metal deposit induces the changes in the structure of the nickel matrix (Fig.3b-f). This means that incorporation of nano-Cr_2O_3 has modified the surface morphology of nickel matrix. It has been shown that Cr_2O_3 nanoparticles influence the competitive formation of nickel nuclei and crystal growth. Cr_2O_3 particles show a distinct tendency to form conglomerates uniformly distributed over the whole surface of the coating. Some of them protrude above the surface of the nickel matrix while other, despite being deeply embedded in it, is not covered by a layer of the metal because of their dielectric properties. This result is agreement with Benea (Benea L. etal. 2001). In addition, to confirm the modified surface morphology of nickel matrix with nano-Cr_2O_3 incorporation, XRD spectra was recorded for the deposited layer containing low and high Cr_2O_3 V_f%. The phase structures of Ni–nano-Cr_2O_3 coating containing various amounts of chromium oxide powder are represented in Fig. 4. The XRD pattern of the Ni–<5V_f% Cr_2O_3 layer (Fig. 4a) showed that the structure of this type exhibits a nickel matrix at different 2θ angles corresponding to the crystalline matrix of the Ni layer. At the same time, Cr_2O_3 peak is observed at Bragg's angles 44.5, while the pattern of the Ni–>5V_f% Cr_2O_3 layer (Fig. 4b) showed only one peak characterized with Cr_2O_3, indicating the embedding of the Cr_2O_3 particles into the nickel matrix changed the crystal structure of nickel from crystalline to amorphous structure. The codeposited nano-particles act as nucleation centers and thus perturbing the nickel growth. Hence, the nano-composite is characterized with an amorphous structure compared to the pure nickel films.

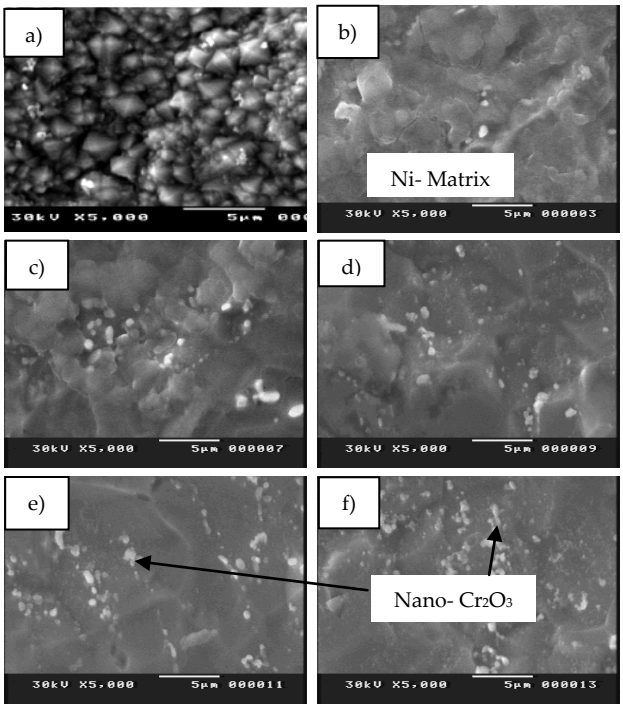

FIG.3. SURFACE MORPHOLOGY OF NI-NANO- Cr_2O_3 COMPOSITE FROM BATHS CONTAINING DIFFERENT Cr_2O_3 CONCENTRATION AND OPERATED AT, 50 °C, pH5, 150 Rpm AND 7 ADM^{-2}, a) Ni- free Cr_2O_3, b) + 5 gl^{-1} Cr_2O_3, c) + 10 gl^{-1} Cr_2O_3, d) + 12gl^{-1} Cr_2O_3, and e) + 15 gl^{-1} Cr_2O_3, f) 20 gl^{-1} Cr_2O_3 .

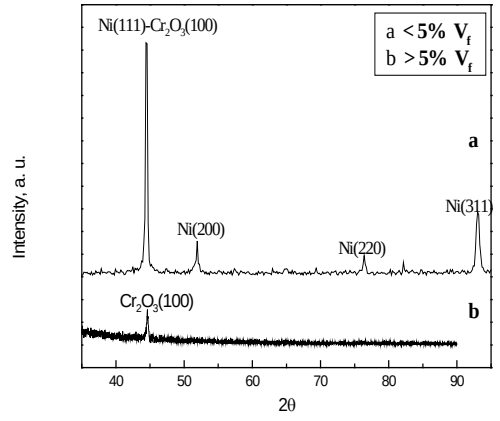

FIG. 4 XRD PATTERN OF NI–CR_2O_3 NANO-COMPOSITE COATING DEPOSITED AT 7 ADM^{-2} PH 5, 150RPM, 50 °C AND CONTAINING DIFFERENT V_F OF NANO- Cr_2O_3, a) < 5 V_f NANO- Cr_2O_3 AND b) >5 V_f NANO- Cr_2O_3

Effect of Stirring Rate

Cr_2O_3 particles should be transported to the cathode surface for the codeposition, so, the stirring rate strongly affects the content of Cr_2O_3 in the deposit. The codeposition of nano-Cr_2O_3 with nickel was carried out at 7 Adm^{-2}, 50 °C, pH 5 and 20 $gl^{-1}$of Cr_2O_3 particles suspended in the plating solution. The influence of stirring rate on V_f% is shown in Fig. 5. The V_f% of Cr_2O_3 increases with stirring rate and reaches a maximum value at 150 rpm, then decreases with the stirring rate. The nano particles are prone to agglomerating together, so at very low stirring rate, the stirring energy is too weak to reduce the agglomerate of powder. As the stirring rate increases, it becomes strong enough to dispersion the nano-Cr_2O_3 particle. So the codeposition of nano-Cr_2O_3 particles increases as the stirring rate increases up to a certain stirring rate (150rpm). In addition, when the stirring rate is smaller than 150 rpm, the codeposition behavior of Cr_2O_3 particles with Ni matrix is apparently controlled by particle transfer while at very rapid stirring rate, collision factor may be the most important reason that causes the decrease in codeposition of Cr_2O_3 particle (Yeh S.H. etal. 1997). Another reason is perhaps that the increasing streaming velocity of the suspension may also dislodge and sweep away the loosely adsorbed Cr_2O_3 particles on the cathode surface, causing a reduction in codeposition.

Effect of Current Density

The current density is also found to influence the amount of Cr_2O_3 nanoparticles incorporated into electrodeposited nickel. Figure 6 shows the effect of current density on the Cr_2O_3 V_f% of composite coatings from bath containing 20 $gl^{-1}$of Cr_2O_3 particles and operated at 50 °C, pH 5 and 150 rpm. It is clear that the V_f% of Cr_2O_3 increases initially with the current density and reaches a maximum at 7Adm^{-2}. Beyond this current density, the V_f% of Cr_2O_3 decreases. The maximum value can be attributed to the transition from an activation controlled metal deposition reaction to a diffusion

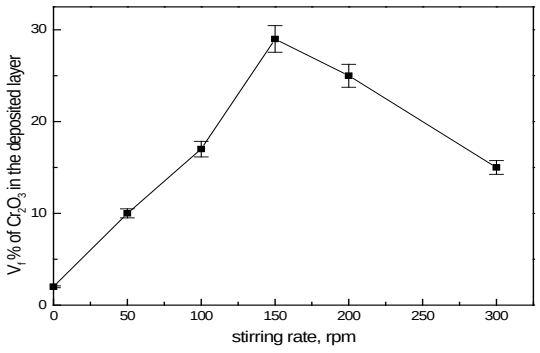

FIG.5 RELATIONSHIP BETWEEN STIRRING RATE AND Vf % OF Cr2O3 IN THE DEPOSITED LAYER OPERATED AT 50 °C, pH 5, 7ADM-2 AND 20 gl-1 Cr2O3.

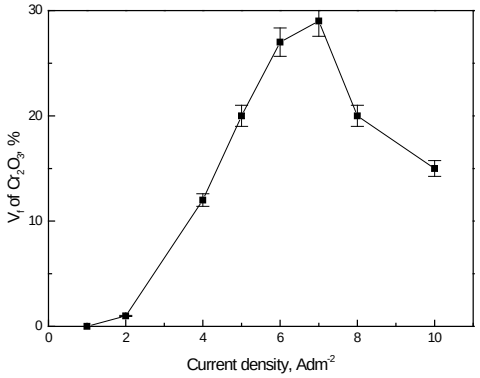

FIG.6 EFFECT OF CURRENT DENSITY ON V_f % of Cr_2O_3 IN THE DEPOSITED LAYER OPERATING AT 50 °C, pH 5, 150 RPM AND 20 gl^{-1} Cr_2O_3.

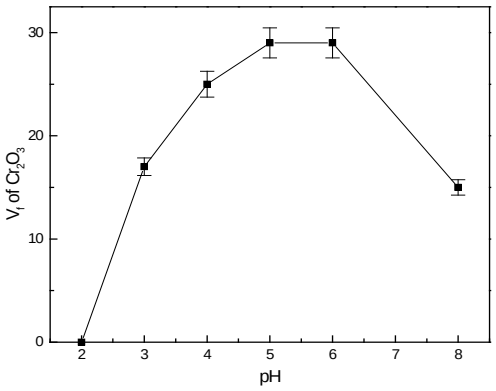

FIG.7 RELATIONSHIP BETWEEN PH OF THE ELECTROLYTE AND Vf % of Cr2O3IN THE DEPOSITED LAYERS OPERATED AT 50 °C, 150 RPM, 7ADM-2 And 20 gl-1 Cr2O3.

controlled of particles transfer. The energy required to deposit metal ions that were solvated and adsorbed on the Cr_2O_3 surface is larger than that for free deposited metal ion (Benea L. etal. 2001). Owing to the difference in activated energy required for deposition, at low current density the codeposition of Cr_2O_3 is low, which may be a result of the preferred free metal ions deposition. While with increasing current density, this energy difference becomes less important, therefore, codeposition of Cr_2O_3 increases. Deposits obtained by applying current densities higher than 7Adm^{-2} were brittle and tended to peel off at the edges of the substrate, probably because of the high current distribution. Therefore, with further increase in the current density, the extent of codeposition of Cr_2O_3 decreases. In addition, at higher current density more than 7Adm^{-2} the loose adsorption of the particles may become rate controlling. Owing to this is slower than the metal deposition rate, incorporation of Cr_2O_3 decreases with increasing in current density.

Effect of pH

The pH value of the electrolyte plays an important role in the codeposition process. Electrolytic codeposition of Cr_2O_3 particle with nickel matrix was operated at 7 Adm^{-2}, 50°C, 150 rpm and 20 $gl^{-1}$of Cr_2O_3 particles suspended in the plating solution. Figure 7 shows the variation of Cr_2O_3 codeposition with pH of the plating bath. As can be seen, the V_f% of Cr_2O_3 increases as increasing pH values and attains the greatest value at pH 5-6. With further increasing pH >6 the V_f% of Cr_2O_3 in the deposited layer decreases due to the formation of nickel hydroxide in alkaline medium which leads to the decrease in the deposition rate and consequently decreasing the V_f% of Cr_2O_3.

The deposition behavior of Cr_2O_3 with pH can be explained by an electrophoresis phenomenon due to the formation of an ionic cloud around the Cr_2O_3 particles. Electrophoresis is the induced motion of colloidal particles or molecules suspended in ionic solutions that result from the application of an electric field. The electrophoretic velocity is a function of the etectrostatic forces on the surface charge, the electrostatic forces on their electric double layers, and the viscous drag associated with the motion of the colloidal particles as well as the motion of the ionic cloud and the colloidal particles. The sign and magnitude of the electrolytic charge is known as zeta potential (ζ). Figure 8 shows the surface charge of Cr_2O_3 particles in NaCl electrolytes at various pH values. It was found that nano-sized Cr_2O_3 particles have negative surface charge at pH > 2 and positive charge at pH ≤2. Therefore, pH ~2.5 is the point of zero charge (PZC). The results indicated that the magnitude of the negative charge of the particles decreases with increasing pH values up to−34 mV at pH 8. The most excellent results were obtained at pH 5 and zeta potential −31 mV due to the adsorption of metal ions on particle surface more useful than that of hydrogen ions. The decrease of H^+ ions concentration in electrolyte contributed to the metal ions adsorption on the surface of the Cr_2O_3 particles, which led to increase in codeposition of Cr_2O_3 with Ni (Szczygiel B. 1997). This means that, the surface charge of the Cr_2O_3 can adsorb Ni^{2+} ions and change the polarity of the Cr_2O_3 from negative to positive in an aqueous solution containing Ni^{2+} ions which accelerates the electrophoretic movement of the Cr_2O_3 particles towards the cathode. The experiment was restricted to pH 5 because the composite layer formed at higher pH

loses its surface brightness and cannot form a dense layer. In addition, zeta potential increases as pH decreases, which is due to the fact that Cr_2O_3 powder has a stronger tendency to absorb H^+ at lower pH values than that to absorb Ni^{2+}.

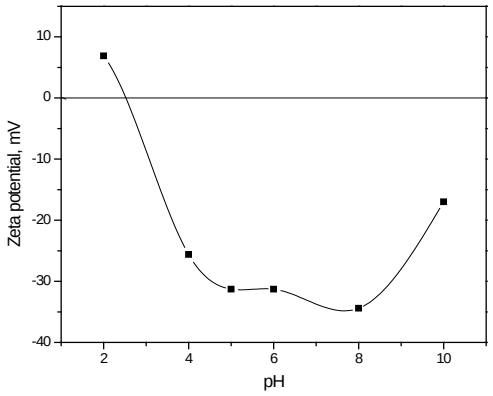

FIG.8 ZETA-POTENTIAL OF Cr_2O_3 PARTICLES WITH PH.

Effect of Temperature

The effect of bath temperature on V_f of Cr_2O_3 in the deposited layer at a fixed Cr_2O_3 concentration in the electrolyte (20 gl^{-1}) and operated at pH 5, 150 rpm and 7 Adm^{-2} is shown in Fig. 9. It was observed that V_f% of Cr_2O_3 increased initially with increasing temperature and reached a maximum at 50°C. The influence of temperature on the Cr_2O_3

incorporation was suggested and confirmed in view of the collision theory in which chemical reaction molecules with a minimum amount of energy to react during collision, which is called the activation energy gained by a molecule to react at temperature 50°C, must collide with each other. Moreover, the maximum observed in the curve of temperature effect can be attributed to the transition from an activation controlled metal deposition reaction to a diffusion controlled particles transfer .

Properties of the Composite Coating

Microhardness Property

The properties of the composite coating are generally related to the presence of solid particles in the deposited layers. The relationship between the Cr_2O_3 incorporation in the deposited layer and hardness is demonstrated in Table 2. The results reveal that the typical hardness values for steel and pure nickel are 140 and 230 HV_{100}, respectively, while the incorporation of Cr_2O_3 particles with nickel matrix confers greatly increased values of microhardness. The incorporation of nano-Cr_2O_3 into nickel deposit led to further increasing in the hardness values up to 750 HV_{100} with 29 V_f % Cr_2O_3 in the coating layer.

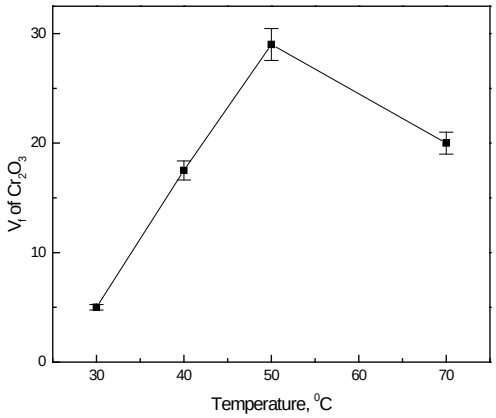

FIG. 9 EFFECT OF TEMPERATURE ON Vf % OF Cr2O3 IN THE DEPOSITED LAYER OPERATED AT pH 5, 150 RPM, 7ADM-2 AND 20 gl-1 Cr2O3.

There are three reasons for the increase in hardness: particle-strengthening, dispersion-strengthening and grain refining mechanisms (Bapu G.R. 1995, Robin A. etal. 2007). In this study the increase of hardness should be attributed to dispersion-strengthening and grain refining mechanisms. It has been reported that the incorporation of the nano-Cr2O3 particles in the deposit as well as the modified structure of the nickel matrix deposit led to improvement in the hardness. This revealed that the incorporation of fine hard particles within the Ni matrix could restrain the growth of Ni crystals and impede the motion of dislocations. These effects become stronger with increasing nano-Cr2O3 contents, and thus increasing the hardness of the Ni matrix composites.

TABLE 2THE RELATIONSHIP BETWEEN THE Cr2O3 INCORPORATION IN THE DEPOSITED LAYER AND MICROHARDNESS

Samples	Hv_{100} ±10
Steel	140
Steel-Ni	230
Steel-Ni- 5 $V_fCr_2O_3$	250
Steel-Ni- 10 $V_fCr_2O_3$	250
Steel-Ni- 15 $V_fCr_2O_3$	375
Steel- Ni- 20 $V_fCr_2O_3$	458
Steel- Ni- 29 $V_fCr_2O_3$	750

Adhesion Property

Adhesion of the Ni-composite layer to the steel substrate deposited at optimum condition (pH 5, 150

rpm, 50°C and 7 Adm− 2) having 29 Vf% Cr2O3 in the coating layer was evaluated using scratch test. High adhesive Ni-composite layer with steel substrate was found. The result of adhesion was confirmed by thermal shock test. The sample was heated at 650°C for 24 hs then quenched into water. Figure 10 shows the morphologies of the coated samples before and after thermal shock tests. After thermal shock (Fig. 9 b) there is no crack or spalling observed on the cross section film surface of Ni–Cr2O3. It is obvious that the films still adhered well to the substrate showing a good adhesion between the Ni–Cr2O3 film and the steel substrate which represents good plating quality without swell and peeling off.

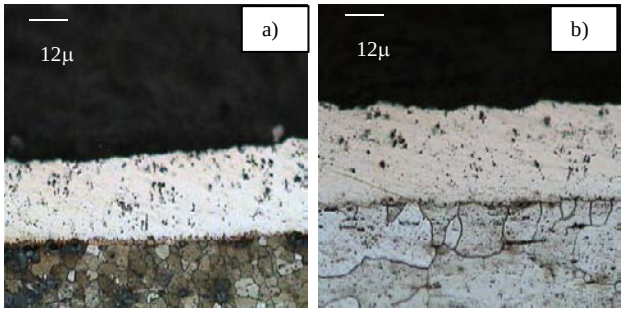

BEFORE THERMAL AFTER THERMAL

FIG.10 THE IMAGES OF THE CROSS SECTION Ni-Cr_2O_3 COATINGS BEFORE AND AFTER THERMAL SHOCK TESTS.

Corrosion Property

An immersion weight loss technique was applied to investigate the corrosion behavior of the mild steel before and after coatings. The tested sample was immersed in 3.5% NaCl at room temperature and the variation of the weight loss with time is shown in Fig. 11. It is perceptible that the weight loss WLoss increased linearly with immersion time for all samples. Zhao has expressed this linear relationship by the following equation (Zhao Q. etal. 2005):

$$W_{Loss}=at+b \quad (1)$$

where a and b are constants for a given sample in a given NaCl concentration. They can be determined by least square technique. The annual corrosion rate γ (mm/year) can be calculated using the following equation:

$$\gamma = a \cdot 365x24/100\rho \quad (2)$$

where ϱ is the density of the steel (gcm-3). Table 3 shows also the comparison of annual corrosion rate of uncoated steel and steel coated with Ni, and Ni–Cr2O3 with different volume fraction of Cr2O3 in 3.5% NaCl solutions.

It is clear from obtained data that the composite coating shows lower corrosion rate compared to uncoated and coated steel with pure nickel. This behavior can be explained in accordance with Z. Abdel Hamid (Abdel Hamid Z etal. 2002), where Cr2O3 particles act as corrosion inhibitor blocking metallic surface properties. The lowest corrosion rate for Ni-29%Vf Cr2O3 was attributed to more distribution and good bonding of the Cr2O3 particles with Ni-matrix. In addition, the annual corrosion rates of Ni–Cr2O3 composite coatings were much lower than those of uncoated and coated steel with Ni. This behavior can be explained on the basis that Cr2O3 particles act as inert physical barriers to the initiation and development of defect corrosion, hence improving the corrosion resistance of the coating.

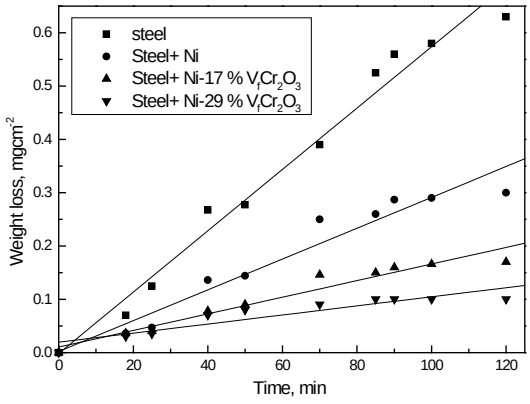

FIG.11. RELATIONHIP BETWEEN IMMERSION TIMES AND WEIGHT LOSS OF UNCOATED AND COATED STEEL WITH PURE NICKEL AND Ni-Cr2O3 .

TABLE 3 COMPARISON OF ANNUAL CORROSION RATE OF UNCOATED STEEL AND STEEL COATED WITH Ni, Ni–Cr2O3 IN 3.5 % NaCl SOLUTIONS

Samples	annual corrosion rate, mpy
Steel	0.07
Steel-Ni	0.033
Steel- Ni- 15 V_f Cr_2O_3	0.018
Steel- Ni-29V_f Cr_2O_3	0.011

CONCLUSIONS

Nano-sized Cr_2O_3 particles were codeposited with Ni by using CEP technique from Watt's bath. The effects

of plating parameters such as pH of the plating bath, Cr_2O_3 concentration in the plating bath, stirring rate, temperature and current density on the deposition behaviors of Ni–Cr_2O_3 composite coating layers were studied. The following conclusions are derived from the present study.

1. The maximum Cr_2O_3 incorporation (~ 29% V_f) could be attained at optimum conditions; 20 $g1^{-1}$ of Cr_2O_3 particles in suspension, 7Adm^{-2}, pH 5, 150 rpm, and 50°C.

2. The codeposition behavior is influenced by the Cr_2O_3 particle charge. The nano-sized Cr_2O_3 particles have negative surface charge at pH > 2 and positive charge at pH ≤2.

3. The morphology of composite coatings has showed that the incorporation of nano-Cr_2O_3 particles changes the surface morphology of nickel matrix.

4. The hardness of nanocomposite coating depends directly on the V_f% of of nano- Cr_2O_3.

5. The Ni- nano- Cr_2O_3 composite coating has lower corrosion rate compared to that of uncoated and coated steel with pure nickel.

REFERENCES

Aal A.A., Ibrahim K.M., Hamid Z.A., Wear, **260** (2006) 1070.

Abdel Aal A., Zaki Z.I. and Abdel Hamid Z., Mater. Sci. Eng. A**, 447** (2007) 87**.**

Abdel Hamid Z. and Abou Elkhair M.T., Mater. Lett. **57** (2002) 720.

Abdel Hamid Z. El-Adly and R.A., Plat. Surf. Finish. **86** (1999) 136.

Abdel Hamid Z. and Ghayad I. M., Mater. Lett., **53** (2002) 238.

Balaraju J.N, Sankara Narayanan T.S.N., and Seshadri S.K., Mater. J. Appl. Electrochem., **33** (2003) 807.

Bapu G.R., Plat. Surf. Finish. **82** (1995) 70.

Benea L., Bonora P. L., Borello A., and Martelli S., Wear, **249** (2001) 995.

Bercot P., Pena-Munoz E. and Pagetti J., J. Surf. Coat. Technol., **157** (2002) 282.

Berkh O., Bodnevas A. and Zahavi J., Plat. Surf. Finish. **82** (1995) 62.

Celis J. P., Roos J.R., Buelens C., And Fransaer J., JOM, **42** (1990) 60.

Celis J. P., Roos J.R, Buelens C., And Fransaer J., Trans. Inst. Met. Finish. **69** (1991)133.

El-Reheim F. H. A., El-Midany A. A. and Selim K. A., Trans. Inst. Min Metall. C, **117,** 3 (2008) 153.

Fransaer J., Celis J.P. , J. Electrochem. Soc., **139** (1992) 413.

Guglielmi N., J. Electrochem. Soc., **119** (1972) 1009.

Hou K. H., Ger M. D., Wang L. M., Ke S. T., Wear**, 253** (2002) 994.

Maurin G., Lavanant A., J. Appl. Electrochem.. **25** (1995) 1113.

Pickering F.B., "The Basic of Quantitative Metallography", North Way House, High Road, Whetstone, London, N 209 LW (1976).

Qiuyuan F., Tingju L., Hongyun Y. Kai, Q., Fudong B. Junze J., Appl. Surf. Sci., **254** (2008) 2262.

Ramesh Bapu G.N.K., Surf. Coat. Technol. **67** (1994) 105.

Robin A., and Fratari R.Q., J. Appl. Electrochem., **37** (2007) 805.

Rossi S., Chini F., Straffelini G., Bonora P.L. Moschini, R. and Stampali A., Surf. Coat. Technol., **173** (2003) 235.

Sarret M., Müller C. and Amell A., Surf. Coat. Technol., **201**, (2006) 389. Shawki S. and Abdel Hamid Z., Aircr. Eng. and Aerosp. Technol. 69 (1997) 432.

Szczygiel B., Plat. Surf. Finish., **84** (1997) 62.

Wahi R.P. and Ilschner B., J. Mater. Sci., **15** (1980) 87.

Yeh S.H., and Wan C.C., "A Study of SiC/Ni Composite Plating in the Watts Bath", Plat. Surf. Finish., **84** (1997) 54.

Zhang C., Ling G. and Li J., Composites A, **36** (2005) 715.

Zhao Q., and Liu Y., Corros. Sci. **47** (2005) 2807.

Zhong-jia H., and Dang-sheng X., Surf. Coat. Technol., **202** (2008) 3208.